

Adsorption of Aromatics from Base Oil over Polymeric Resins: Equilibrium and Kinetics

Mariana Busto,* Jorge H. Sepulveda, Nicolás R. Carrara, and Carlos R. Vera

Instituto de Investigaciones en Catálisis y Petroquímica (INCAPE), Facultad de Ingeniería Química (FIQ), Universidad Nacional del Litoral (UNL)–Consejo Nacional de Investigaciones Científicas y Técnicas (CONICET), Santiago del Estero 2654, S3000AOJ Santa Fe, Argentina

ABSTRACT: Adsorption of aromatic molecules from base oil over an acid resin (Amberlyst 15W) was studied, with a focus on reducing the aromatic content to that of a white mineral oil. It was found that the adsorption capacity of the resin was low. At saturation in the best condition, the adsorption capacity corresponded to 10% acid capacity. The effects of dilution, temperature, and adsorption time were studied. In the absence of a diluting solvent, the isotherm was unfavorable and the adsorption rate was low, with a pseudo-first-order constant of about 0.1 h^{-1} . Dilution of the oil with *n*-hexane had beneficial effects on the adsorption capacity, the adsorption rate, and the yield of refined oil. The 1:1 (vol/vol) dilution was found to be optimal. Kinetic data were better explained by a model of dominant intraparticle diffusion, with the adsorbate load being proportional to the square of the adsorption time. Dilution with *n*-hexane was thought to decrease the viscosity with a proportional increase of the diffusivity and a decrease of the chemical affinity of the oil matrix. Estimations of the oil purity and refined oil yield after a series of equilibrium stages indicated that three stages with an adsorbent/oil ratio of 0.5 (g g^{-1}) and a 1:1 dilution in *n*-hexane could refine the studied base oil (initial aromatic content of $0.136 \text{ mmol g}^{-1}$) to a white mineral oil of food grade, with a yield of about 60%. Removal of the solvent was considered easy given the high volatility of *n*-hexane compared to that of the oil.

1. INTRODUCTION

White mineral oil is a specialty oil obtained from the refining of crude oil that is mainly used in pharmacopeia, cosmetics, and the food industry. This kind of application dictates that white mineral oil should have a reduced or null content of aromatic hydrocarbons, sulfur, and nitrogen. White mineral oils comprise mixtures of hydrocarbons with 18 or more carbon atoms and a boiling range between 280 and 600 °C.¹ They are usually produced by refining of base oils coming from extraction units.

The white mineral oil is classified into two classes according to its use: the technical grade for cosmetics, textile, lubrication, insecticides, etc. [as defined in FDA 21 CFR 178.3620(b)] and one more highly refined, used in the formulations of drugs, food, and non-food articles in contact with food [as defined in FDA 21 CFR 172.878 and FDA 21 CFR 178.3620(c)]. The white mineral oil must be chemically inert, colorless, odorless, and tasteless. According to the United States Food and Drug Administration (FDA) regulation 21 CFR 172.878, pharmacopeia-grade oil must meet a limit of ultraviolet (UV) absorptivity of 0.1 (for 1 cm optical path) in the range of wavelengths (λ) between 260 and 350 nm.² This UV limit translates to an almost null concentration of aromatics.

The classical methodology to obtain white mineral oil is hydrodesulfuration, dearomatization, and hydroisomerization.^{3–6} For hydrotreatment, the usual catalysts are Ni–Mo/ Al_2O_3 or Ni–W/ Al_2O_3 .^{7–9} The process requires a high hydrogen pressure (50–100 kgf cm^{-2}) depending upon the aromatic amount.^{10,11} Older techniques involve treatment with oleum to form aromatic sulfones that are then eliminated by extraction and adsorption.¹² This route produces inconvenient amounts of toxic wastes and requires carefully controlled reaction conditions, especially the control of the temperature,

to prevent the formation of unwanted products that might reduce the yield of the refined product.

Because both sulfonation and hydrotreatment routes can prove inconvenient to small-scale producers of white mineral oil, other routes should be suggested. In this work, we assess the dearomatization of base oils to produce white mineral oils by means of adsorption. Adsorption techniques do not demand high pressures or the handling of hazardous chemicals. In this sense, they are simpler and safer than hydroisomerization or sulfonation. Some papers in the literature can be found related to the adsorption of aromatics and polyaromatics of diesel^{13–18} or aqueous streams.^{19,20} Different adsorbents have been used, such as zeolites,^{15,21} Al_2O_3 ,¹⁶ and activated carbon.^{13,14,17,18,22}

Choosing an optimal adsorbent for any application demands characterization of its adsorption capacity, selectivity, regenerability, adsorption rate, and cost. Rarely a single adsorbent can be optimal regarding all of these aspects. In this work, we studied the feasibility of using a commercial macroporous cation-exchange resin for the dearomatization of mineral oils. Commercial resins have good properties of thermal and chemical stabilities, are easily regenerated, and have an open pore structure that minimizes mass-transfer problems. Particularly, we studied the use of a macroporous Amberlite 15W resin, in the form of 0.6–0.85 mm beads, with an average pore size of 30 nm. The focus was put on the influence of the temperature, dilution, and contact time. Thermodynamic and kinetic constants were obtained, and the feasibility of practical dearomatization by this technique was discussed.

Received: September 19, 2014

Revised: January 12, 2015

Published: January 13, 2015



2. EXPERIMENTAL SECTION

2.1. Materials and Methods. 2.1.1. Adsorbent Conditioning.

Before the adsorption experiments or the characterization tests, the resin was washed to remove all traces of dispersant agents. These agents have UV signals at 270 nm, which interfere with the measurement of aromatics in oil. Several washes with distilled water and methanol were performed until the washing solution had no UV signal. The washed resin was then immersed in 10 wt % sulfuric acid solution for 2 h and flushed with water until the pH of the outlet solution was almost the same as pure water according to Leung.²²

2.1.2. Characterization. The total capacity of the exchange resin in the H⁺ form was obtained by neutralization with it with a sodium salt to displace hydrogen from the surface. The free protons were subsequently titrated as free acidity.^{23–26}

2.1.3. Adsorption Equilibrium and Kinetic Tests. Both equilibrium adsorption and adsorption kinetics tests were carried out at three different temperatures (40, 60, and 80 °C). The base oil used (base oil 60) was generously supplied by YPF SA (Dirección Lubricantes y Especialidades América, Buenos Aires, Argentina). The concentration of aromatics of this oil was 118 mmol L⁻¹. This was expressed in equivalent benzene moles per unit volume, and it was measured by adding growing aliquots of benzene, measuring the UV absorption at 254 nm and extrapolating to zero absorbance. These and other properties of the base oil are indicated in Table 1.

Table 1. Base Oil Feedstock Properties

property	method	amount
density at 20 °C (g cm ⁻³)	gravimetry/volumetry	0.863
viscosity at 40 and 80 °C (poise)	ASTM D445	15.658 and 4.621
UV absorbance at 230, 270, and 310 nm	ASTM D2269	2, 0.4, and -
aromatic content (mmol _{Bz} L ⁻¹)	benzene addition	118
aromatic content (mmol g ⁻¹)		0.136
boiling range (°C)	ASTM D7500-08	285–565
carbon number	SimDis/comparison to <i>n</i> -paraffin standards	18–40

For adsorption isotherms and kinetic tests, a packed bed with liquid recirculating flow was used. The adsorbent was packed in the middle of a stainless-steel column of 9 mm internal diameter and 20 cm height, fixed by means of stainless-steel mesh, and recirculated through the packing by means of stainless-steel 1/8 in. tubing and a Watson-Marlow Qsci400 peristaltic pump. The liquid flow was 5.6 mL min⁻¹. For adsorption isotherms, the oil volume was kept constant (25 mL) and the adsorbent mass was varied. For the kinetics test, the relation of adsorbent/oil was kept constant at 0.32. The adsorbent was used in its original particulate form, i.e., without further milling. After the solution was stabilized, an aliquot was taken and diluted with *n*-hexane (Merck, 99.99%) and the UV absorbance was measured. The aromatic content was read as equivalent benzene millimoles per liter (mmol_{Bz} L⁻¹) against a calibration curve.

All UV absorption measurements were performed in a Shimadzu UV1800.²⁷ UV-vis light was produced by a laser source [deuterium (D₂) lamp and tungsten halogen (WI) lamp], and the wavelength was varied by means of 190–800 nm. The cell was made of polyethylene and had a volume of 1 cm³ and an optical path of 1 cm. The spectra were collected in a computer and analyzed with the UVProbe software.

Runs with diluted base oil were always performed with a solution of the base oil in *n*-hexane (Cicarelli, 95%). In most cases, a volume ratio of *n*-hexane/oil of 1:1, 2:1, and 3:1 was used.

2.1.4. Calculations. The concentration of adsorbate on the solid was determined by means of the mass balance of the liquid phase, before the addition of the solid adsorbent and after adsorption has occurred (eq 1). In conditions of equilibrium, the same equation applies with $q = q_e$ and $C = C_e$. C_e and q_e are the concentrations of the

adsorbate in the liquid and solid at equilibrium conditions, respectively.

$$q = \frac{W_{\text{oil}}(C_0 - C)}{W_{\text{ads}}} \quad (1)$$

Implicit in eq 1 is the assumption of the diluted system, i.e., the transfer of adsorbate molecules to the solid-phase results in a negligible change of W_{oil} . Calculations for adsorption equilibrium stages were made using an equilibrium isotherm formula (eq 2), e.g., Langmuir's formula, and the equation for the adsorbent/oil ratio R (eq 3). The final nonlinear equation (eq 4) was solved for each equilibrium stage using a Levenberg–Marquardt algorithm implemented in the software MatLab for Windows (fsolve routine).

$$q_e = f(C_e) \quad (2)$$

$$R = \frac{W_{\text{ads}}}{W_{\text{oil}}} \quad (3)$$

$$Rf(C_e) - C_0 + C_e = 0 \quad (4)$$

3. RESULTS AND DISCUSSION

The properties of the oil base stock are detailed in Table 1. The measured properties of the adsorbent (Amberlyst 15W resin) are indicated in Table 2. A calibration curve made by

Table 2. Properties of the Macroreticular Resin Used (Amberlyst 15W)

property	method	amount
type of resin	aromatic, sulfonated styrene–divinylbenzene	
hydrophobicity	hydrophobic	
BET surface area (m ² g ⁻¹)	nitrogen adsorption	52
average pore diameter (nm)	nitrogen adsorption	30
pore volume (cm ³ g ⁻¹)	nitrogen adsorption	0.40
particle size (wet mesh) (μm)	screening	<300
acid (mmol g ⁻¹)	master test method	3.40
particle density (g cm ⁻³)		1.50
particle porosity (cm ³ cm ⁻³)		0.45
solid density (g cm ⁻³)		2.73
bed density (g cm ⁻³)	gravimetry and volumetry	0.77
bed porosity (cm ³ cm ⁻³)		0.48

incremental addition of benzene can be seen in Figure 1. The original content of aromatics (in equivalent benzene concentration) can be obtained by extrapolation to zero.

Amberlyst 15 in either its dry or wet form is known to be a mild solid acid with sulfonic acid groups attached to aromatic nuclei. Fourier transform infrared spectroscopy (FTIR) characterization data have been recently reported by Ordonsky et al.²⁸ A band at 1176 cm⁻¹ would result from the symmetric stretching vibration of the sulfonic groups, and the band at 1123 cm⁻¹ was assigned to the in-plane skeletal vibration of the disubstituted benzene ring. Bands at 1034, 1004, and 829 cm⁻¹ were attributed to the in-plane skeletal vibration of the disubstituted benzene ring. The bands at 1034, 1004, and 829 cm⁻¹ were attributed to the in-plane bending vibration of a phenyl ring substituted with a sulfonic acid group. A broad band at 3350 cm⁻¹ was attributed to the stretching of hydrogen-bonded OH groups. Siril et al.²⁹ measured the acidity of sulfonic acid on polymeric supports and concluded that the acid strength of the sulfonic acid followed the order: Nafion H > Amberlyst 35 > Amberlyst 15. Ammonia on

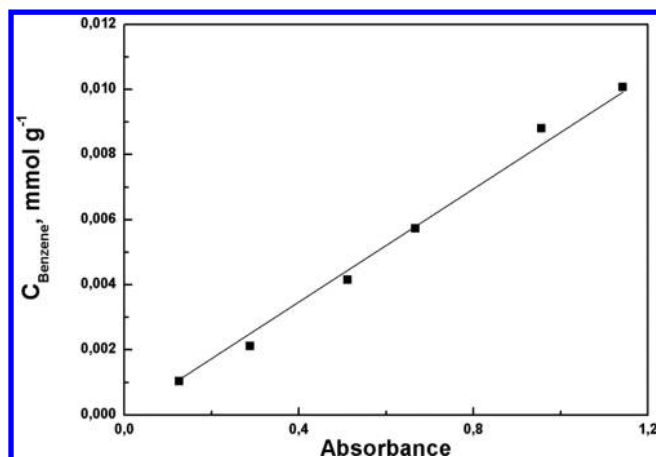


Figure 1. Calibration curve for measuring the amount of aromatics in the base oil.

Amberlyst 15 showed an enthalpy of adsorption of 25–30 kJ mol⁻¹ and a saturation capacity of 4.7 mmol g⁻¹. The latter coincides with the number of exchangeable acid sites reported by the supplier. It must however be noted that this number varies widely in the case of the wet resin because of the base weight used in the calculation. We have measured a value of 3.4 mmol g⁻¹, and Ordonsky et al.²⁸ measured a value of 2.6 mmol g⁻¹.

3.1. UV–Vis Calibration Curve. A calibration curve was made by adding successive aliquots of benzene and measuring the UV–vis spectrum. Inspection of the spectrum for different solution samples indicated that the best wavelength for analysis was 254 nm. Then, a plot was made of the absorbance as a function of the additional benzene content. The original aromatic content of the oil (in equivalent benzene concentration units) was obtained by extrapolation of the plot line to zero absorbance. Shifting the line to the right to make it pass through the zero point yields the final calibration curve, with UV–vis absorbance as a function of the aromatic content, expressed in equivalent benzene millimoles per gram (see Figure 1).

3.2. Adsorption Equilibrium Isotherms. Equilibrium isotherms at 40 and 60 °C corresponding to the adsorption of aromatics from the pure base oil and over the resin adsorbent are plotted in Figure 2. Another isotherm at 40 °C was obtained using diluted oil (1:1, vol/vol) and also included in Figure 2. The shape of the isotherms for the pure oil (undiluted) found was seemingly unfavorable. Some isotherm models were fitted, and model parameters were obtained. The models are those depicted in eqs 5–8.^{30,31} Values of the fitted parameters are detailed in Table 3. For the pure oil, the Langmuir model gave wrong estimates for the characteristic constants (<0), while the Freundlich model gave the best fit. According to McKay et al.³² Freundlich's *n* values greater than 1 are typical of systems with favorable isotherms, while those with *n* < 1 would have unfavorable isotherms. The latter is the case of the resin–(pure oil) systems. For the diluted oil, the isotherm is transformed into a favorable isotherm (*n* = 3.2). For this system, the best fit is obtained with Langmuir's model.

$$q_e = \frac{Q_0 b C_e}{1 + b C_e} \quad (\text{Langmuir}) \quad (5)$$

$$q_e = K_F C_e^{1/n} \quad (\text{Freundlich}) \quad (6)$$

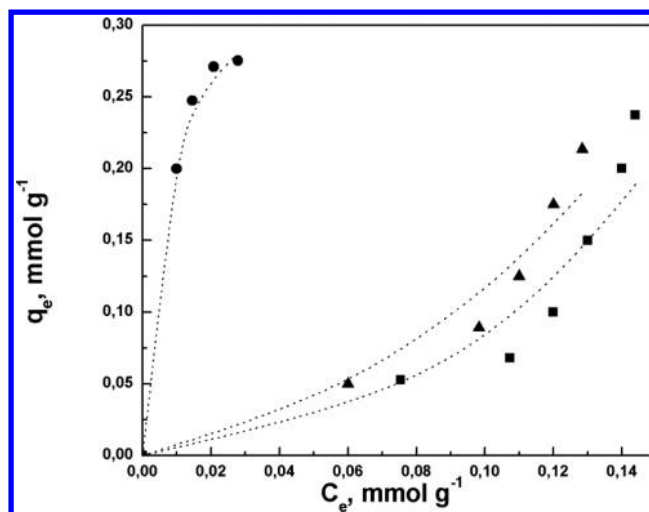


Figure 2. Equilibrium isotherms: (■) 40 °C, pure oil; (▲) 60 °C, pure oil; and (●) 40 °C, diluted oil (1:1, vol/vol). C_e of the diluted system has been calculated without considering the presence of the diluent, i.e., with the concentration of aromatics in millimoles per gram of oil (ignoring the diluent). Dotted line = model fit.

Table 3. Parameter Values Corresponding to Different Isotherm Models

isotherm model	system	parameter value	r^2
Langmuir	40 °C, pure	$Q_0 = 3.695$ $b = -0.04667$	0.9799
	60 °C, pure	$Q_0 = -0.072$ $b = -5.83292$	0.98036
	40 °C, diluted	$Q_0 = 0.346$ $b = 154.78$	0.9883
Freundlich	40 °C, pure	$K_f = 16.56$ $n = 0.433$	0.8479
	60 °C, pure	$K_f = 7.79$ $n = 0.547$	0.9231
	40 °C, diluted	$K_f = 0.879$ $n = 3.20$	0.8842
Temkin	40 °C, pure	$A = 14.3$ $B = 0.2628$	0.7558
	60 °C, pure	$A = 19.74$ $B = 0.1918$	0.7871
	40 °C, diluted	$A = 1667.6$ $B = 0.0742$	0.9032
Dubinin–Radushkevich	40 °C, pure	$k_{ad} = 0.0008$ $q_s = 1.762$	0.8152
	60 °C, pure	$k_{ad} = 0.0005$ $q_s = 1.096$	0.8999
	40 °C, diluted	$k_{ad} = 0.00006$ $q_s = 0.4768$	0.9076

$$q_e = \frac{R_g T}{B} \ln(AC_e) \quad (\text{Temkin}) \quad (7)$$

$$q_e = q_s e^{(-k_{ad} e^2)} \quad (\text{Dubinin–Radushkevich}) \quad (8)$$

For Langmuir's isotherm, the value of Q_0 indicates the theoretical saturation capacity of the adsorbent. We can see that, for the diluted system, this is 0.346 mmol g⁻¹. Considering the total amount of acid sites (3.4 mmol g⁻¹) and the maximum adsorbate load of Figure 1 (about 0.28 mmol g⁻¹), it turns out that the number of occupied sites corresponds to 8.2% of the

total number of sulfonic groups. In this sense, we are supposing that adsorption is likely being produced in this case by the attraction between the sulfonic acid group of the resin and the aromatic nucleus of the alkyaromatic that would be acting in this case like a Lewis base.

The change in the isotherm shape upon dilution can be due to a change in the adsorbate–fluid and adsorbate–solid interactions. Without dilution in *n*-hexane, the affinity between the aromatic molecules and the oil molecules seems to be greater than the interaction between the adsorbate molecules and the solid. This affinity could arise from the interaction between the long alkyl chains of the oil matrix and long alkyl substituents present in the aromatic molecules. Upon dilution with *n*-hexane, this interaction could be decreased.

For a given adsorbent, the interaction with the adsorbate depends upon the properties of the solid, with such forces as van der Waals forces, hydrophilic/hydrophobic interactions, and hydrogen bridge being important.³³ The basic functional group of the resin is the aromatic sulfonic group. The cation of this group is usually a H⁺ proton. In the case of the adsorbate, the alkyl aromatic molecule, the aromatic ring has an alkyl substituent that produces an electron induction effect that increases the electron density of the ring. This high electron density inhibits the formation of hydrogen bridge bonds with the OH groups of the resin.

The low percentage of sulfonic groups used for the adsorption hints that there are some negative factors acting. This, in principle, could simply be the high activity of the alkyl aromatic adsorbate in the oil. Another possible factor is the lipophobic nature of the surface. Roschina et al.³⁴ indicate that the adsorption of an organic compound over a polar surface, such as that of the exchange resin, can be hampered by the limited wetting of the surface.

3.3. Calculation of Equilibrium Stages. Considering a series of equilibrium stages, it is important to calculate the number of adsorption stages needed to convert the base oil into a white mineral oil with the quality level required by the U.S. FDA 172.878 standard (aromatic concentration yielding a value of 0.1 of absorbance per centimeter of optical path). The results for such a treatment using a diluted feed [1:1 (vol/vol) in *n*-hexane] are plotted in Figure 3. The equilibrium parameters of the Langmuir isotherm for the diluted system are used ($Q_0 = 0.346 \text{ mmol g}^{-1}$ and $b = 154.78 \text{ g mmol}^{-1}$). Each operation line corresponds to a different resin/oil ratio.

It is considered that, after adsorption is finished, the resin is filtered with a net loss equal to the bed interstitial volume and the pore volume of the resin. The yield in Figure 4 is the fraction of the original oil mass that is recovered at the end of the treatment. It can be seen that, with $R = 0.5$ and three equilibrium stages, the recovered oil almost complies with the U.S. FDA quality standard. This treatment would have a net yield of almost 60%. The discarded oil volume can be recovered by flushing the resin with a solvent. A hot stream of oil/solvent should also help to remove the adsorbed aromatics.

The beneficial effect of dilution cannot be overstressed. Dilution with *n*-hexane not only improves the capacity of adsorption of the resin but also decreases the losses during filtration of the resin, in successive batch equilibrium stages. Supposing that the interstitial volume and the pore volume are lost, eq 9 should be applied. It can be seen in this equation that the effect of dilution (D) is that of reducing the relative amount of oil (and solvent) trapped in the resin. For $R = 0.5$ and $D = 0.5$ [1:1 (vol/vol) dilution], the yield after one equilibrium

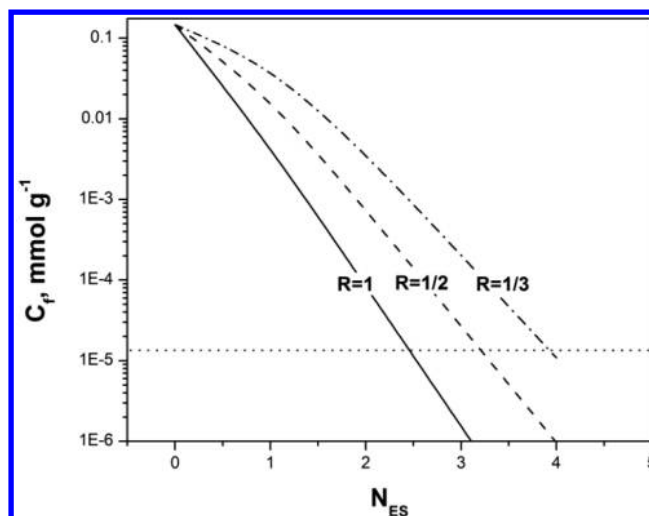


Figure 3. Residual aromatic concentration (C_f) as a function of the number of equilibrium stages (N_{ES}) and the resin/oil ratio (R , g g^{-1}). Dotted line = residual concentration dictated by the U.S. FDA 172.878 standard (aromatic concentration producing a value of 0.1 absorbance per centimeter of optical path). The diluted oil is 1:1 (vol/vol) in *n*-hexane. C_f is related to the undiluted oil.

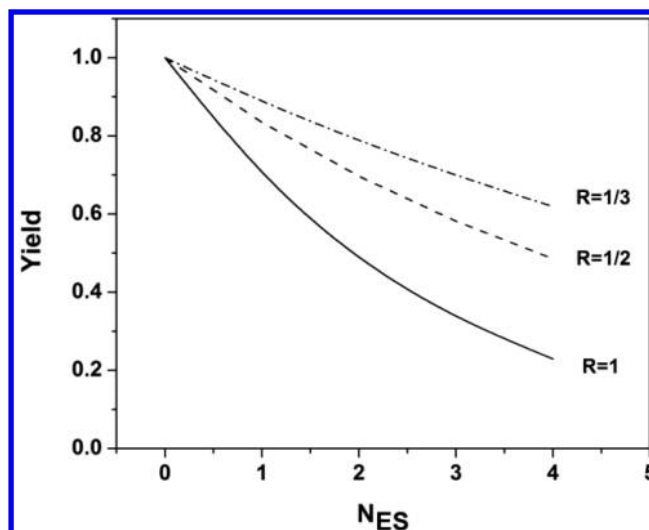


Figure 4. Yield as a function of the number of equilibrium stages. Diluted oil is 1:1 (vol/vol) in *n*-hexane.

stage is $Y = 0.83$. Increasing the dilution to $D = 0.333$ [1:2 (vol/vol) dilution] increases the yield to $Y = 0.89$.

$$Y = 1 - \frac{(\varepsilon_{\text{bed}} + (1 - \varepsilon_{\text{bed}})\varepsilon_{\text{particle}})\left(\frac{R}{\rho_{\text{bed}}}\right)}{\left(\frac{1}{D\rho_{\text{oil}}}\right) + \left(\frac{R}{\rho_{\text{solid}}}\right)} \quad (9)$$

However, dilution also has some drawbacks. These would be (i) the need for moving bigger volumes of solution with the associated higher pumping costs and bigger storage vessels and (ii) the need for separating the solvent from the oil by evaporation, stripping, or distillation.

3.4. Adsorption Kinetics. The effect of the contact time on the degree of dearomatization of the oil was studied under varying conditions of the temperature (40, 60, and 80 °C) and dilution (pure and 1:1, 2:1, and 3:1 volumetric dilutions). The results related to the kinetics at different temperatures are

plotted in Figure 5. The pattern of variation is not monotonic. Increasing the temperature from 40 to 60 °C increases the rate

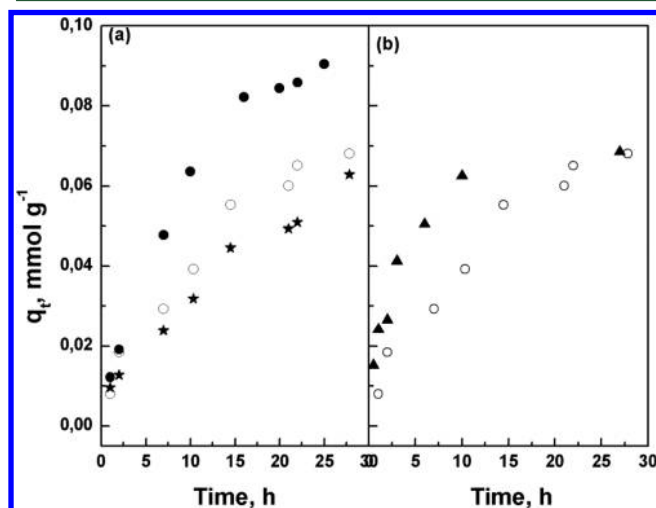


Figure 5. Adsorbed amount of aromatics as a function of time and temperature of a system of pure (undiluted) base oil and Amberlite 15W resin, with $C_0 = 0.136 \text{ mmol g}^{-1}$ and $R = 0.32 \text{ g g}^{-1}$: (a) (●) 40 °C, (○) 60 °C, and (★) 80 °C, with particle size = 300 μm , and (b) (○) 300 μm and (▲) 152 μm , with temperature = 40 °C.

by about 20% (steeper slope in the 0–15 h range), while increasing it to 80 °C produces no practical variation in the rate.

For the value of C_0 and R and using the Freundlich isotherm at 40 °C, $q_{\text{eq}} = 0.106 \text{ mmol g}^{-1}$, while using the Freundlich isotherm at 60 °C, $q_{\text{eq}} = 0.099$. This means that, at 30 h and 60 °C, the surface has practically reached saturation, while at 40 °C, only 60% of the saturation value is reached. The increase in the adsorption rate when increasing the temperature from 40 to 60 °C was expected. However, at 80 °C, adsorption decreases seemed rare. The non-monotonic pattern could be the result of the combination of a kinetic effect, the higher rate at higher temperatures, and a thermodynamic effect, the lower capacity at higher temperatures.

In any case, it is clear that the rate of adsorption is very low in all cases. Taking a pseudo-first-order model (see eq 11), the pseudo-first-order constant k is about 0.1 h^{-1} . It can be seen that the effect of dilution is again beneficial. In comparison to the pure, undiluted oil (Figure 6), the adsorption rate is increased 6 times when diluting 1:1 in *n*-hexane. Higher dilution ratios do not increase the adsorption rate or the final equilibrium amount of adsorbed aromatics. The higher adsorption rate upon dilution can be primarily due to a decrease in the viscosity of the oil that, in turn, produces an increase in the molecular diffusivity of the adsorbate, as predicted by the Stokes–Einstein equation.

$$D_{\text{ST}} = \frac{k_1 T \rho_{\text{solution}}}{6\pi r \mu} \quad (10)$$

The effect of the decrease in the adsorption rate upon further dilution of the oil can be due to the decrease in the driving force for adsorption, C , because of the dilution.

The adsorption process consists of three successive steps: (a) diffusive transport of aromatic molecules from the bulk of the feed to the surface of the resin particles through the boundary layer (film diffusion), (b) intraparticle diffusion through the

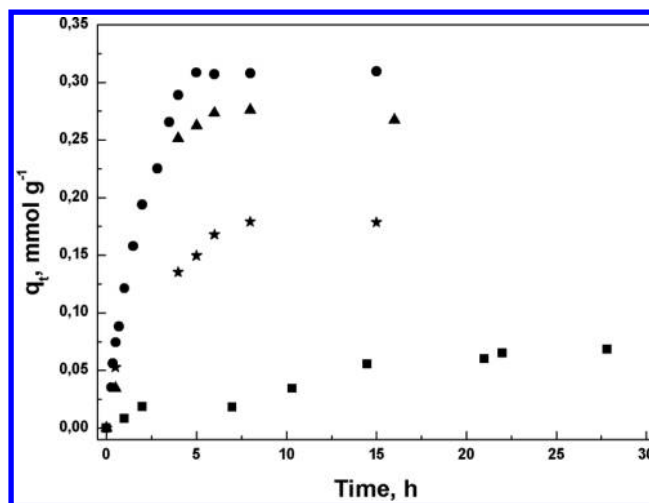


Figure 6. Effect of dilution on the rate and capacity for adsorption of aromatics from base oil, with the temperature of 40 °C and *n*-hexane as the diluent (*n*-hexane/oil solution): (■) pure, undiluted oil, (●) 1:1 (vol/vol), (▲) 2:1 (vol/vol), and (★) 3:1 (vol/vol), with $C_0 = 0.136 \text{ mmol g}^{-1}$ (diluent not considered) and $R = 0.32 \text{ g g}^{-1}$.

inner pores of the resin, and (c) adsorption of the aromatic molecules on the surface of the resin. The temperature has an opposite effect on diffusion (steps a and b) and adsorption (step c). It favors the external and internal mass transfer because of the increase of the molecular diffusivity. For adsorption, the opposite effect is seen because most adsorption processes are exothermal. To determine which of the steps controlled the kinetics of adsorption of the system under study, several models were tried, which are depicted below.^{35,36} The results of the fitting of the data of Figure 5 are detailed in Table 4.

$$\frac{dq_t}{dt} = k_1(q_e - q_t) \quad (\text{pseudo-first-order model}) \quad (11)$$

$$\frac{dq_t}{dt} = k_2(q_e - q_t)^2 \quad (\text{pseudo-second-order model}) \quad (12)$$

$$\frac{dq_t}{dt} = a \exp(-b_E q_t) \quad (\text{Elovich model}) \quad (13)$$

$$q_t = k_{\text{id}} t^{0.5} + C_{\text{id}} \quad (\text{intraparticle diffusion model}) \quad (14)$$

The results seem to indicate that the kinetics are dominated by intraparticle diffusion because this model fits the data better. The intraparticle diffusion model assumes that the film diffusion is negligible, and the intraparticle diffusion is the only rate-controlling step. This model can be derived from Fick's second law under two assumptions: first, the intraparticle diffusivity D_{id} is constant; second, the uptake of adsorbate by the solid is small relative to the total quantity of adsorbate present in the solution. k_{id} ($\text{mmol g}^{-1} \text{ h}^{-0.5}$) is defined as the intraparticle diffusion rate constant and is related to the intraparticle diffusivity as in eq 15.

$$k_{\text{id}} = \frac{6q_e}{R_g} \sqrt{\frac{D_{\text{id}}}{\pi}} \quad (15)$$

Table 4. Comparison of the Pseudo-First-Order, Pseudo-Second-Order, Elovich, and Intraparticle Diffusion Models for the Resin–(Pure Oil) System at Different Temperatures

model	T (°C)/dilution	q_e , a , and k_{id}	k_1 , k_2 , b , and C_{id}	r^2
pseudo-first order	40/pure	0.0773	0.1244	0.9215
	60/pure	0.0980	0.1409	0.9888
	80/pure	0.0596	0.0723	0.9838
pseudo-second order	40/pure	0.0959	0.8780	0.9431
	60/pure	0.1302	0.7117	0.9897
	80/pure	0.0821	0.9739	0.8922
Elovich	40/pure	0.0040	54.945	0.9411
	60/pure	0.0057	38.610	0.9763
	80/pure	0.0032	65.789	0.9028
intraparticle diffusion	40/pure	0.0144	−0.0049	0.9796
	60/pure	0.0204	−0.0067	0.9807
	80/pure	0.0117	−0.0028	0.9830
	40/1:1	0.1629	−0.0442	0.9963
	40/2:1	0.1443	−0.0613	0.9953
	40/3:1	0.0651	0.0061	0.9985

The value of C_{id} in eq 14 reflects the effect of the film thickness. If the q versus $t^{0.5}$ plot is linear and passes through the origin, intraparticle diffusion is supposed to be the rate-limiting step. If not, then intraparticle diffusion might not be the only limiting step.³⁷ The value of C_{id} is approximately zero, and then it seems that adsorption of aromatics from the undiluted oil is dominated by diffusion inside the resin particles.

A further assessment of the importance of the film mass transfer can be performed by evaluating the Biot number (eq 16). Estimates of both the diffusivity and the film transfer coefficient are needed in this equation. The film mass-transfer coefficient can be estimated using the Wilson and Geankoplis correlation for mass transfer in a packed bed (eq 17).

$$Bi = \frac{k_f d_e}{D_{id}} \quad (16)$$

$$Sh = \frac{1.09}{\epsilon_b} Sc^{0.33} Re_p^{0.33} = \frac{d_p k_f}{D_M} \quad (17)$$

$$Sc = \frac{\mu}{\rho D_M} \quad (18)$$

$$Re_p = \frac{\rho V d_p}{\mu} \quad (19)$$

In these equations, V is the interstitial velocity, Sh is the Sherwood number, Sc is the Schmidt number, and Re_p is the particle Reynolds number. Other symbols correspond to the fluid density (ρ), the fluid viscosity (μ), and the molecular diffusivity of the adsorbate in the fluid (D_M). Using the properties of the fluid and resin, as indicated in Tables 1, 2, and 5, estimates of D_M and k_f can be obtained along with values of

Table 5. Variation of Density and Viscosity of the Feed

T (°C)/dilution	density (g cm ^{−3})	viscosity (g cm ^{−1} s ^{−1})
40/pure	0.8465	15.66
60/pure	0.8364	8.61
80/pure	0.8195	4.62
40/1:1	0.6916	1.179
40/2:1	0.6809	0.637
40/3:1	0.6810	0.523

the Biot number. These are detailed in Table 6 for the case of the pure undiluted oil at three different temperatures. The obtained molecular diffusivity values (D_M) are similar to those reported by Luna et al.³⁸

Table 6. Estimates of the Molecular Diffusivity, Film Transfer Coefficient, and Biot Number for the Resin–(Pure Oil) System at Three Different Temperatures

system	T (°C)	D_{id} (cm ² s ^{−1})	k_f (cm s ^{−1})	Bi
pure	40	3.42×10^{-7}	8.52×10^{-4}	80.3
pure	60	3.89×10^{-7}	1.32×10^{-3}	110
pure	80	4.04×10^{-7}	2.09×10^{-3}	167
diluted 1:1	40	2.13×10^{-6}	3.05×10^{-3}	46.1
diluted 2:1	40	2.11×10^{-6}	4.39×10^{-3}	67.2
diluted 3:1	40	1.12×10^{-6}	4.93×10^{-3}	142

As a rule, intraparticle mass transfer controls the adsorption rate at $Bi > 50$ and film diffusion controls the adsorption rate at $Bi < 0.5$. In the intermediate range, both mechanisms are relevant for the overall adsorption rate. In accordance with the results of Table 6, only intraparticle diffusion is important. The effect of dilution is thus seemingly that of reducing the intraparticle diffusivity.

The presence of this diffusion problem can be verified by inspecting the plots of Figure 5b. Reducing the particle size effectively increases the rate of adsorption while not affecting the final equilibrium value.

4. CONCLUSION

Adsorption of aromatic molecules from base oil and on an acid resin was studied. The adsorption capacity of the resin was low, lower than 0.3 mmol g^{−1}. In the absence of a diluting solvent, the isotherm was unfavorable and the adsorption rate was low, with a pseudo-first-order constant of about 0.1 h^{−1}. Dilution of the oil with *n*-hexane had beneficial effects on the adsorption capacity, the adsorption rate, and the yield of refined oil. A 1:1 (vol/vol) dilution was found to be optimal, with higher dilutions being detrimental to the adsorption rate and capacity.

Estimations of the oil purity and refined oil yield after a series of equilibrium stages indicated that three stages with an adsorbent/oil ratio of 0.5 (g g^{−1}) and a 1:1 dilution in *n*-hexane could refine the studied base oil (initial aromatic content of

0.136 mmol g⁻¹) to a white mineral oil of food and pharmacopeia grade, with a yield of about 60%. Removal of the solvent was considered easy given the high volatility of *n*-hexane compared to that of the oil.

The system exhibited Freundlich isotherms in the undiluted state and Langmuir isotherms in the diluted state. Kinetic data were well-fitted by a model of dominant intraparticle diffusion, with the adsorbate load being proportional to the square of the adsorption time. Dilution with *n*-hexane was thought to influence the system in two ways: a decrease in viscosity with a parallel increase of the diffusivity and a decrease of the affinity of the oil matrix.

AUTHOR INFORMATION

Corresponding Author

*Telephone: +54-342-4533858. E-mail: mbusto@fiq.unl.edu.ar.

Notes

The authors declare no competing financial interest.

ACKNOWLEDGMENTS

This work was financially supported by CONICET (PIP 0235), ANPCyT (PICT 1685), and Universidad Nacional del Litoral (CAI+D Grant 50120110100323).

NOMENCLATURE

- a = initial adsorption rate (Elovich model) (mmol g⁻¹ h⁻¹)
 A = Temkin isotherm equilibrium binding constant (g mmol⁻¹)
 b = Langmuir's constant (g mmol⁻¹)
 b_E = Elovich constant (g mmol⁻¹)
 B = Temkin isotherm constant
 Bi = Biot number ($k_f R/D$)
 C = liquid-phase concentration (mmol g⁻¹)
 C_0 = initial bulk liquid-phase concentration (mmol g⁻¹)
 C_{eq} = equilibrium liquid-phase concentration (mmol g⁻¹)
 C_f = residual aromatic concentration (mmol g⁻¹)
 C_{id} = intraparticle diffusion model constant (mmol g⁻¹)
 d_e = equivalent diameter (cm)
 d_p = particle diameter (cm)
 D = volumetric ratio of oil/*n*-hexane
 D_0 = surface diffusivity at zero surface coverage (cm² s⁻¹)
 D_{id} = diffusivity defined in eq 15 (cm² s⁻¹)
 D_M = molecular diffusivity of the adsorbate in the fluid (Wilke–Chang equation) (cm² s⁻¹)
 D_s = surface diffusivity (cm² s⁻¹)
 k_1 = pseudo-first-order model constant (h⁻¹)
 k_2 = pseudo-second-order model constant (g mmol⁻¹ h⁻¹)
 k_{ad} = Dubinin–Radushkevich isotherm constant (mmol² kJ⁻²)
 k_{id} = intraparticle diffusion model constant (mmol g⁻¹ h^{-0.5})
 k_f = film mass-transfer coefficient (cm s⁻¹)
 K_F = Freundlich isotherm constant (mg/g)
 n = adsorption intensity (Freundlich isotherm)
 N_{ES} = number of equilibrium stages
 q_t = solid-phase concentration (mmol g⁻¹)
 q_{eq} = solid-phase adsorbate concentration in equilibrium with the bulk liquid concentration
 C_{eq} = liquid-phase adsorbate concentration in equilibrium with the solid concentration
 q_s = theoretical isotherm saturation capacity (mmol g⁻¹)
 Q_0 = saturation capacity of the adsorbent (mmol g⁻¹)
 r = adsorbent particle radius (cm)

R = resin/oil ratio (g g⁻¹)

Re_p = Reynolds number

R_g = universal gas constant (kJ mol⁻¹ K⁻¹)

Sc = Schmidt number

Sh = Sherwood number

t = time (s)

T = temperature (K)

V = interstitial velocity (cm s⁻¹)

W_{ads} = mass of adsorbent (g)

W_{oil} = mass of oil (g)

Y = fraction of the oil mass is recovered at the end of the treatment

ϵ = Dubinin–Radushkevich isotherm constant

ϵ_{bed} = bed porosity (cm³ cm⁻³)

$\epsilon_{particle}$ = particle porosity (cm³ cm⁻³)

ρ_{bed} = bed density (g cm⁻³)

ρ_{oil} = oil density (g cm⁻³)

$\rho_{solution}$ = *n*-hexane/oil solution density (g cm⁻³)

ρ_{solid} = solid density (g cm⁻³)

μ = feed viscosity (g cm⁻¹ s⁻¹)

REFERENCES

- Hulse, M.; Klan, M. J.; Noreyko, J. M.; Reitman, F. A.; Skisak, C. M.; Smith, J. H.; Tietze, P. G.; Vernot, E. H. *API Mineral Oil Review*; American Petroleum Institute: Washington, D.C., 1992.
- United States Food and Drug Administration (FDA). *Food Additives Permitted for Direct Addition to Food for Human Consumption. Code of Federal Regulations, Part 178, Title 21, 2014; Sec. 178.3620 Mineral Oil*; U.S. FDA: Silver Spring, MD, 2014.
- Kirk, M. C., Jr. Process for producing high pure oil by hydrogenation of dewaxed raffinate. U.S. Patent 3,673,078, June 27, 1972.
- Harrington, P. J. Solvent treating of mineral oils. U.S. Patent 2,298,791, Oct 13, 1942.
- Ul'yanenki, V. I.; Yur'eva, N. P.; Sergeev, V. P. *Chem. Technol. Fuel Oils* **1986**, 22, 214–217.
- Kachmar, O. S.; Bodan, A. N.; Kachmar, B. V.; Kopchick, P. D. *Chem. Technol. Fuel Oils* **1984**, 20, 435–438.
- Mills, I. W.; Dimeler, G. R.; Chester, W. Making white oil by hydrogenation with a sulfided nickel and molybdenum catalyst. U.S. Patent 3,959,122, May 25, 1976.
- Eijsbouts, S.; Anderson, G. H.; Bergwerff, J. A.; Jacobi, S. *Appl. Catal., A* **2013**, 458, 169–182.
- Speight, J. G. *The Refinery of the Future*; Gulf Professional Publishing, Elsevier, Oxford, U.K., 2011.
- Lucien, J.; Dutot, G. Process for the preparation of a lubricating base oil. U.S. Patent 4,906,350 A, March 6, 1990.
- Hantzer, S. S.; Joseck, E. D.; Hilbert, T. L.; Ruibal, E. A.; Andre, J.-P. L.; Palmer, T. R.; Carroll, M. B. All catalytic medicinal white oil production. U.S. Patent 7,594,991 B2, Sept 29, 2009.
- Nussbaum, M. L.; Knaggs, E. A. Of petroleum feedstock. U.S. Patent 4,148,821, April 10, 1979.
- Bu, J.; Loh, G.; Gwie, C. G.; Dewiyanti, S.; Tasrif, M.; Borgna, A. *Chem. Eng. J.* **2011**, 166, 207–217.
- Seredych, M.; Bandosz, T. J. *Fuel Process. Technol.* **2010**, 91, 693–701.
- Oliveira, M. L. M.; Miranda, A. A. L.; Barbosa, C. M. B. M.; Cavalcante, C. L., Jr.; Azevedo, D. C. S.; Rodriguez-Castellon, E. *Fuel* **2009**, 88, 1885–1892.
- Jeevanandam, P.; Klabunde, K. J.; Tetzler, S. H. *Microporous Mesoporous Mater.* **2005**, 79, 101–110.
- Fallah, R. N.; Azizian, S.; Reggers, G.; Carleer, R.; Schreurs, S.; Ahenach, J.; Meynen, V.; Yperman, J. *Fuel Process. Technol.* **2014**, 119, 278–285.
- Arcibar-Orozco, J. A.; Rangel-Mendez, J. R. *Chem. Eng. J.* **2013**, 230, 439–446.

- (19) Li, A.; Zhang, Q.; Zhang, G.; Chen, J.; Fei, Z.; Liu, F. *Chemosphere* **2002**, *47*, 981–989.
- (20) Yuan, M.; Tong, S.; Zhao, S.; Ji, C. Q. *J. Hazard. Mater.* **2010**, *181*, 1115–1120.
- (21) Hernández-Maldonado, A. J.; Yang, R. T. *AIChE J.* **2004**, *50*, 791–801.
- (22) Leung, P. Hydration of isobutene in trickle bed reactors. Ph.D. Thesis, University of California, Davis, Davis, CA, 1986.
- (23) Helfferich, F. *Ion Exchange*; McGraw Hill: New York, 1962; pp 87–91.
- (24) Kunin, R. *Ion Exchange Resins*; Robert Kreiger Publishing Company: Malabar, FL, 1985.
- (25) Gregor, H. P.; Hamilton, M. J.; Becher, J.; Bernstein, F. *J. Phys. Chem.* **1955**, *59*, 874–881.
- (26) Fisher, S.; Kunin, R. *J. Phys. Chem.* **1956**, *60*, 1030–1032.
- (27) ASTM International ASTM D-2269. *Standard Test Method for Evaluation of White Mineral Oils by Ultraviolet Absorption*; ASTM International: West Conshohocken, PA, 2010.
- (28) Ordonsky, V. V.; Schouten, J. C.; van der Schaaf, J.; Nijhuis, T. A. *Chem. Eng. J.* **2012**, *207–208*, 218–225.
- (29) Siril, P. F.; Davison, A. D.; Randhawa, J. K.; Brown, D. R. *J. Mol. Catal. A: Chem.* **2007**, *267*, 72–78.
- (30) Limousin, G.; Gaudet, J.-P.; Charlet, L.; Szenknect, S.; Barthès, V.; Krimissa, M. *Appl. Geochem.* **2007**, *22*, 249–275.
- (31) Foo, K. Y.; Hameed, B. H. *Chem. Eng. J.* **2010**, *156*, 2–10.
- (32) McKay, G.; Blair, H. S.; Gardner, J. K. *J. Appl. Polym. Sci.* **1982**, *27*, 3043–3057.
- (33) Yang, R. T. *Adsorbent: Fundamentals and Applications*; Wiley-Interscience: Hoboken, NJ, 2003.
- (34) Roshchina, T. M.; Shonija, N. K.; Bernardoni, F.; Fadeev, A. Y. *Langmuir* **2014**, *30*, 9355–9360.
- (35) Qiu, H.; Lv, L.; Pan, B.-C.; Zhang, Q.-J.; Zhang, W.-M.; Zhang, Q.-X. *J. Zhejiang Univ., Sci., A* **2009**, *10*, 716–724.
- (36) Weber, W. J.; Morris, J. C. Advances in water pollution research: removal of biologically resistant pollutants from waste waters by adsorption. *Proceedings of the International Conference on Water Pollution Symposium*; Pergamon Press: Oxford, U.K., 1962; Vol. 2.
- (37) Vadivelan, V.; Kumar, K. V. *J. Colloid Interface Sci.* **2005**, *286*, 90–100.
- (38) Luna, F. M. T.; Pontes-Filho, A. A.; Trindade, E. D.; Silva, I. J.; Azevedo, D. C. S.; Cavalcante, C. L. *Ind. Eng. Chem. Res.* **2008**, *47*, 3207–3212.